International Journal of Nanoelectronics and Materials
IJNeaM
ISSN 1985-5761 | E-ISSN 2232-1535

# Density Functional Theory Study on the Reactivity and Stability of Calix[n]arene-paba Complexes: Drug Sensor Application

Yeong Yi Wong [a], Faridah Lisa Supian [a]*, Afiq Radzwan [a], Nur Farah Nadia Abd Karim [a], Amiruddin Shaari [b], and Aminu Shehu Yamusa [b c]

[a]*Department of Physics, Faculty of Science and Mathematics, Sultan Idris Education University, Tanjong Malim, 35900, Malaysia*
[b]*Department of Physics, Faculty of Science, University of Technology Malaysia, Skudai, 81310, Malaysia*
[c]*Federal College of Education, Zaria, 810282, Nigeria*
** Faridah Lisa Supian. Tel.: +60123094418; e-mail: faridah.lisa@fsmt.upsi.edu.my*

Received 14 March 2023, Revised 13 July 2023, Accepted 6 October 2023

**ABSTRACT**

As drug carriers, calixarenes are often investigated and employed in numerous sectors as host molecules. The use of calixarenes in drug delivery systems is a relatively new notion, despite the fact that countless studies have been conducted on calixarenes and their various applications. It is worthwhile to research the computational investigation of the host-guest interaction between calixarenes and para-aminobenzoic acid (PABA) in terms of their binding energy and band gap. The first principles study of PABA sensing by calix [4] arene (C4) and calix [6] arene (C6) based on density functional theory (DFT) was carried out in this study using Quantum ESPRESSO software. By using the computational method, the binding energy, as well as the band gap of C4, C6, PABA, and the novel complexes, C4-PABA, and C6-PABA, were calculated. Different interaction distances were used in the formation of complexes. Our results demonstrate the reduction of the band gap for both complexes. Furthermore, the calculated binding energy shows the promising stability of the complexes. This demonstrates the sensing ability of calixarenes towards PABA and the potential anti-cancer properties of calixarene-PABA in sunscreens.

**Keywords:** *Calixarenes, Band gap, Binding energy, Density functional theory, PABA*

## 1. INTRODUCTION

Understanding the host-guest interaction between a host molecule and a drug, followed by developing the corresponding drug sensor, is vital for future benefits. Calixarenes belong to a family of macrocycles with different phenol units linked by methylene [1]. They are named calix[n]arene, where n represents the number of phenol units. For example, calixarenes with four phenol units and six phenol units are named calix[4]arene and calix[6]arene, respectively [2]. A typical calix[4]arene with four phenol units is shown in Figure 1 [3]. Calixarenes are shaped like a cup with a defined hydrophobic upper rim and a hydrophilic lower rim, together with a hydrophobic cavity. The unique structure and properties of calixarenes make them capable of holding different substances, including ions and neutral molecules [4], [5]. This contributes to the outstanding sensing ability [6], [7]. Their capability to form host-guest complexes contributes to numerous fields, including cosmetic, medical, and pharmaceutical applications [8], [9].

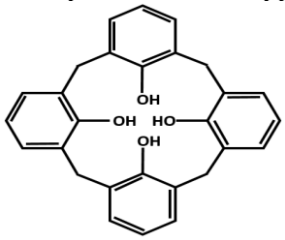


**Figure 1** Chemical structure of a typical calix[4]arene

In this study, calix[4]arene (C4) and calix[6]arene (C6) as the host molecules are used as sensing materials, whereas *para*-aminobenzoic acid (PABA) is targeted to be detected. PABA, also named 4-aminobenzoic acid, is an organic compound found naturally in the human body. It is found in the folic acid vitamin and consists of a benzene ring with the amino and carboxyl groups, as shown in Figure 2 [10]–[12]. PABA has been studied as a drug and contributes to various applications due to its pharmaceutical and biological properties, including personal care and cosmetic products [13]–[15]. However, the detrimental side effect of using PABA as the main ingredient in sunscreen has been proven, which are photoallergic dermatitis and allergic contact dermatitis [16]–[18]. Besides, PABA can potentially cause cancer after being exposed to the sun. The carcinogenic potential of PABA is associated with the genetic damage caused by PABA to the DNA, which may stimulate the construction of skin cancer cells [19]. The unique properties of PABA made them worthy of being studied in this work as a guest molecule.

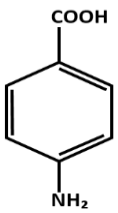


**Figure 2** Chemical structure of a PABA molecule

The host-guest interaction has been studied using different experimental methods, such as host-guest inclusion and the Langmuir technique, followed by experimental characterization [20], [21]. In contrast to those conventional approaches, a computational method based on first-principles density functional theory (DFT) is applied in this study. Based on quantum mechanical modeling, the electronic and structural properties of a material or complex can be calculated and investigated [22], [23]. This work applies DFT to study the host-guest interaction between C4 and C6 as host molecules and PABA as guest molecules, respectively. Their interactions are studied in terms of binding energy and band gaps.

Binding energy is the amount of energy required to break the particles' system into individual parts [24]. The binding energy is considered in this work due to its indication of the stability of a structure or complex. When the binding energy is more negative, the complex is considered more stable due to the stronger interaction [25], [26]. The application of DFT in studying the binding energy of a complex is crucial, especially regarding drug molecules for future benefits [27]. On the other hand, the band gap concept is significant for understanding a material's electrical properties [28]. A band gap is the energy gap between the valence and conduction bands with zero electronic states [29], [30]. The conductivity of a structure, whether the structure is a conductor, semiconductor, or insulator, can be known by studying the band gap [31], [32]. In the band gap study, the density of states (DOS) is the number of states that electrons are allowed to occupy at an energy level [33]. The contribution of each atom present in a structure, for example, carbon (C), hydrogen (H), nitrogen (N), and oxygen (O) involved in this work, can be determined [34]. Besides, the reactivity of the interaction is indicated by the changes in the band gap [35]. The decrease in band gap for a host-guest interaction denotes that the host molecules can stabilize the encapsulated guest molecules via non-covalent interaction. This indicates that the structures involved in the interaction reactwith each other when the band gap is reduced [36].

Calixarenes, as host molecules, are frequently studied and applied in various fields as drug carriers. Despite numerous previous kinds of research regarding calixarene in its different applications, the use of calixarenes in drug delivery systems is still a relatively novel concept. The computational study of host-guest interactions between calixarenes and PABA regarding their binding energy and band gap is worth investigating. In this study, the sensing of PABA using C4 and C6 is studied in terms of binding energy and band gap. This investigates the reactivity and stability of these host and guest molecules. The detection of PABA, even in a very low concentration, is crucial due to its carcinogenic potential. Furthermore, the formation of calixarene-PABA complexes in this work is expected to be applied to prevent cancer caused by sunscreen products. In the coming days, the results obtained in this study could be utilized in various applications, including in the medical and pharmaceutical fields.

## 2. MATERIAL AND METHODS

Free Quantum ESPRESSO software was used as a tool to apply DFT in this study computationally. Based on the first principles calculation, the geometry optimization followed by self-consistent field (SCF) and density of states (DOS) was carried out. The optimized structures with the lowest total energy were used for every DFT calculation. Generalized Gradient Approximation (GGA) in the form of Perdew-Burke-Ernzerhof (PBE) was used to perform the optimization based on the Born-Oppenheimer approximation [37]. The electron-ion core interactions of all atoms, which were carbon (C), oxygen (O), hydrogen (H), and nitrogen (N), were treated by ultrasoft pseudopotentials [38]. Figure 3 below demonstrates the interactive structure of C4, C6, and PABA displayed in Quantum ESPRESSO.

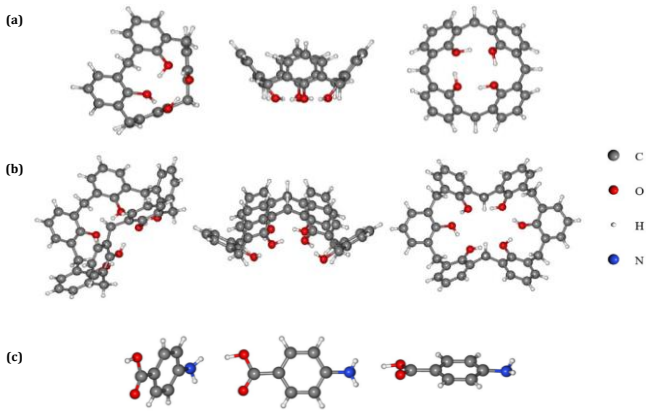


**Figure 3** The interactive structure of (a) C4, (b) C6, and (c) PABA in different dimensions with the C, O, H, and N atoms represented by the grey, red, white, and blue balls, respectively

### 2.1. Computational Details of Density Functional Theory (DFT) Calculation

The binding energy of the structures was computed based on Equation 1 after the optimization calculation, as shown below [39], [40].

$$\Delta E = E_{Calix[n]arene-PABA} - E_{Calix[n]arene} - E_{PABA} \qquad (1)$$

where $E_{Calix[n]arene-PABA}$, $E_{Calix[n]arene}$ and $E_{PABA}$ were the ground state energy of the calix[n]arene, PABA, and calix[n]arene-PABA (n=4,6), respectively.

The band gap for every structure was obtained by performing the SCF calculation. For PABA, 2×1×1 k-points were used for sampling the Brillouin zone for SCF calculation. The cut-off energiesof 25 Ry and 225 Ry were used for the electron wave functions and charge density, respectively. The Gaussian smearing technique was used to perform DOS calculations using 4×3×2 k-points to sample the Brillouin zone. On the other hand, for C4, C6, and the novel complexes constructed using both calixarenes and PABA, as illustrated in Figure 4, 1×1×1 k-points were used for sampling the Brillouin zone for SCF calculation. The cut-off energy similar to PABA was used for the electron wave functions and charge density as well. The Gaussian

smearing technique was also used to perform DOS calculations using 1×1×1 k-points to sample the Brillouin zone.

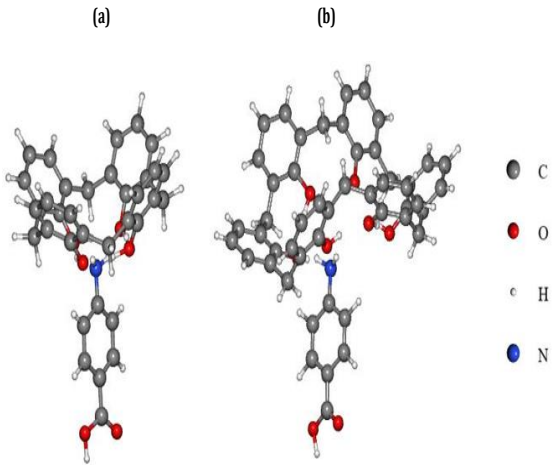


**Figure 4** The interactive structure of (a) C4-PABA and (b) C6-PABA complexes with the C, O, H, and N atoms represented by the grey, red, white, and blue balls, respectively

A 1:1 stoichiometric ratio was used for both C4-PABA and C6-PABA. The use of this ratio was based on the previous research made by Sanku, Karakus, Ilies, and Ilies [41] regarding the 1:1 complex formed by C4 and C6 as the small host. The study by Wang, Ding, and Guo [42] showed that the role of O located at the lower rim of calixarenes was crucial in the interaction between calixarenes and guest molecules. Thus, different interaction distances were adjusted between the PABA and the lower rim of calixarenes to form the corresponding complexes in this work. The bond length was based on the interaction distance between the host and guest molecules [43]. The binding energy was calculated based on the optimized structure of C4-PABA and C6-PABA. The most stable complex with the shortest bond length and highest energy was considered since the greater the energy, the greater the interaction and the greater the sensitivity [44], [45]. The steps were repeated to form the C6-PABA complexes.

## 3. RESULTS AND DISCUSSION

By adjusting the interaction distance, the energy of each complex was used to calculate the binding energy. According to Equation 1, the binding energy for each complex was calculated considering the optimization energy of PABA (-171.5850 Ry), C4 (-474.6038 Ry), and C6 (-711.9134 Ry). The values of binding energy and band gap for C4-PABA and C6-PABA complexes are shown in Table 1 and Table 2, respectively.

### 3.1. Binding Energy

The positive and negative binding energies obtained in this study show the capability of both calixarenes and PABA in the formation of complexes. The positive binding energy suggests an unfavorable and weak interaction, or the formation of an unstable complex between calixarenes and PABA [25], [46], [47]. On the other hand, the negative binding energy indicates a favorite spontaneous reaction with the formation of a stable complex [47]–[49]. Based on the values of binding energy for each C4-PABA complex, the existence of a favorable interaction between C4 and PABA starts at 2.0884 Å. Besides, the formation of stable complexes by C6 and PABA starts at 7.5408 Å. The host-guest interaction indicated by the magnitude of energy increases when the interaction distance decreases, and the stability of the corresponding complex formed is getting greater. This behavior is in good agreement with the previous research made by [44].

By the way, the binding energy of -0.0074 Ry at the shortest distance between the reacted molecules, which is the bond length of 1.8056 Å and -0.0070 Ry at 1.1006 Å, is considered to compare the stability of the complex for C4-PABA and C6-PABA, respectively. This is because the formation of the most stable complex is demonstrated by the most negative binding energy [50]. Furthermore, the negative values of binding energy suggest a promising sensing ability of C4 and C6 towards PABA. Thus, the formation of the stable C4-PABA and C6-PABA complexes in this study could be applied for PABA drug sensors and skin cancer prevention, as discussed in the previous section.

Based on the results shown in Table 1 and Table 2, the binding energies of the most stable C4-PABA and C6-PABA formed are -0.0074 Ry and -0.0070 Ry, respectively. The results show that C4 is capable of forming a more stable complex with PABA compared to C6. This is in good agreement with the previous study made regarding the host-guest interaction of calixarenes, which found that the stability of host-guest complexes formed by calix[4]arene is greater compared to other calixarenes due to its stable conformation [51]. Its outstanding stability is contributed by its small geometry, which performs a delicate spatial control [52].

### 3.2. Band Gap and Density of States (DOS)

The last complexes listed in Table 1 and Table 2 are used in the band gap comparison since these complexes are considered to have the greatest stability. The reactivity between C4 and C6 with PABA molecules is demonstrated by the band gap energy of PABA, C4, C6, and their complexes shown in Table 3.

The results show that the band gap of the C4-PABA complex is smaller than that of pure C4 and PABA molecules. The reduction of the band gap happens to the C6-PABA complex as well. This demonstrates the capability of both C4 and C6 to form complexes with PABA molecules with promising reactivity [36]. The reactivity is in good agreement with the results of their binding energy since a spontaneous and favorable reaction is indicated by a negative binding energy [48]. The reactivity between these host and guest molecules suggests a promising sensing ability of C4 and C6 towards PABA. Thus, the formation of the stable C4-PABA and C6-PABA complexes in this study could be utilized for PABA sensors and skin cancer prevention, as discussed in the previous section.

**Table 1** Binding energy and band gap correspond to the interaction distance of C4 and PABA

| No. | Interaction distance of C4 and PABA (Å) | Optimization Energy (Ry) | Binding Energy (Ry) | Highest Occupied Level (eV) | Lowest Unoccupied Level (eV) | Band Gap (eV) |
|---|---|---|---|---|---|---|
| 1 | 15.4561 | -646.1876 | 0.0013 | -5.2216 | -1.8218 | 3.3998 |
| 2 | 10.0183 | -646.1876 | 0.0013 | -5.2465 | -1.8118 | 3.4347 |
| 3 | 2.0884 | -646.1895 | -0.0006 | -4.6334 | -1.1858 | 3.4476 |
| 4 | 2.0172 | -646.1899 | -0.0010 | -4.6936 | -1.1939 | 3.4997 |
| 5 | 1.8739 | -646.1950 | -0.0069 | -4.2497 | -1.8174 | 2.4323 |
| 6 | 1.8561 | -646.1957 | -0.0069 | -4.2158 | -1.2612 | 2.9546 |
| 7 | 1.8344 | -646.1958 | -0.0070 | -4.1855 | -1.2704 | 2.9151 |
| 8 | 1.8056 | -646.1963 | -0.0074 | -4.0954 | -1.2875 | 2.8079 |

**Table 2** Binding energy and band gap correspond to the interaction distance of C6 and PABA

| No. | Interaction distance of C6 and PABA (Å) | Optimization Energy (Ry) | Binding Energy (Ry) | Highest Occupied Level (eV) | Lowest Unoccupied Level (eV) | Band Gap (eV) |
|---|---|---|---|---|---|---|
| 1 | 13.8333 | -883.4952 | 0.0033 | -5.1408 | -1.7417 | 3.3991 |
| 2 | 8.3381 | -883.4953 | 0.0032 | -5.1617 | -1.7206 | 3.4411 |
| 3 | 7.5408 | -883.4989 | -0.0005 | -4.4470 | -0.9937 | 3.4533 |
| 4 | 4.8276 | -883.4993 | -0.0009 | -4.4712 | -0.9450 | 3.5262 |
| 5 | 1.6057 | -883.5033 | -0.0049 | -4.2408 | -0.7750 | 3.4658 |
| 6 | 1.5345 | -883.5051 | -0.0067 | -4.0871 | -0.7412 | 3.3459 |
| 7 | 1.1485 | -883.5054 | -0.0069 | -3.7449 | -0.7560 | 2.9889 |
| 8 | 1.1006 | -883.5054 | -0.0070 | -3.4149 | -0.7714 | 2.6435 |

**Table 3** Band gap and Fermi energy of PABA, C4, C6, and their complexes

| Structures | Highest Occupied Level (eV) | Lowest Unoccupied Level (eV) | Band Gap (eV) | Fermi Energy (eV) |
|---|---|---|---|---|
| PABA | -4.6101 | -1.0540 | 3.5561 | -2.262 |
| C4 | -4.8912 | -1.2049 | 3.6863 | -3.346 |
| C6 | -4.5736 | -0.7162 | 3.8574 | -2.087 |
| C4-PABA | -4.0954 | -1.2875 | 2.8079 | -2.852 |
| C6-PABA | -3.4149 | -0.7714 | 2.6435 | -1.642 |

However, the band gap is underestimated in this computational study due to the use of the Perdew-Burke-Ernzerhof (PBE) exchange-correlation functional [53]. The actual band gap for insulating materials could be up to 50 % higher than these computational values [54], [55]. The underestimation of the band gap shows that all of the structures in Table 3 are considered insulators when referring to the threshold of 3.0 eV to 3.5 eV [56]. In addition, the Fermi energy shown in Table 3 is located within the band gap, indicating that PABA, C4, C6, and their complexes are insulating [57]. Both the band gap and Fermi energy results are in good agreement with the previous research regarding the conductivity of calixarenes, which shows that calixarenes are a typical insulating material [58], [59].

Overall, the band gap values of C4-PABA demonstrated by the last four complexes with larger interaction distances show a greater reduction than pure C4 and PABA molecules. This shows that the reactivity of host-guest interaction between C4 and PABA increases with the decrease in interaction distance. This is supported by the previous study, which found that decreased distance between the host-guest complex contributes to the strengthened interaction [60]. The same behavior is shown by C6-PABA, where the last two complexes with larger interaction distances denote a larger band gap reduction compared to pure C6 and PABA molecules. Furthermore, the band gap reduction obtained in this work suggests the existence of charge transfer interaction between the host and guest molecules, which means successful complex formation by calixarenes and PABA [61]. By the way, the reduced change in band gap shown by the C4-PABA and C6-PABA, indicating the increase in conductivity, might be studied in the future to explore their potential application beyond drug sensors [31].

The density of states (DOS) for each molecule and complex is studied in terms of the total density of states (TDOS) and the partial density of states (PDOS) to understand the nature of the bands [62]. The TDOS and PDOS of PABA, C4, C6, and their complexes are shown in Figures 5, 6, 7, 8, and 9, respectively. In the figures below, the s and p orbitals of

the C, N, and O are labeled as -s and -p, whereas H shows its only electron-occupied s orbitals.

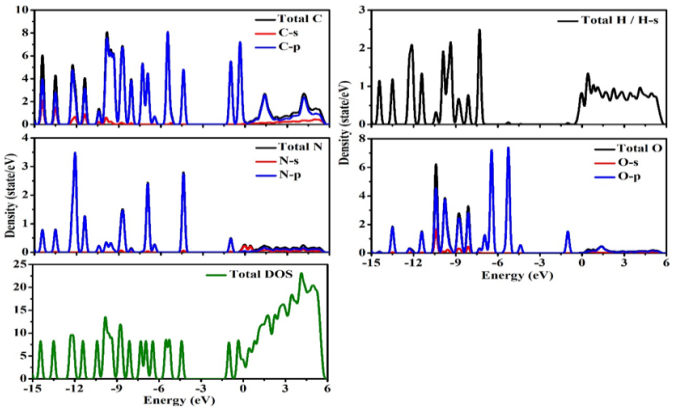


**Figure 5** TDOS and PDOS of PABA

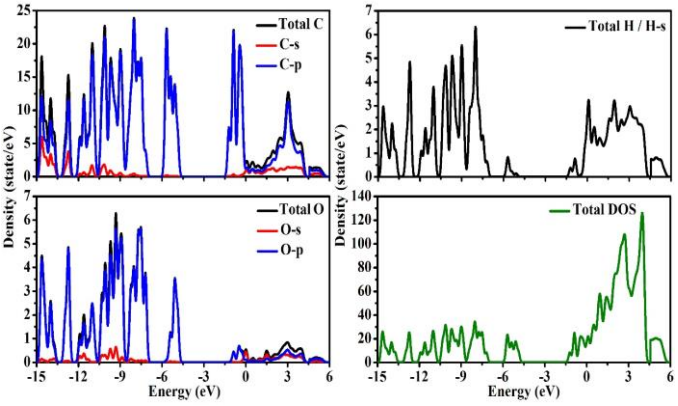


**Figure 6** TDOS and PDOS of C4

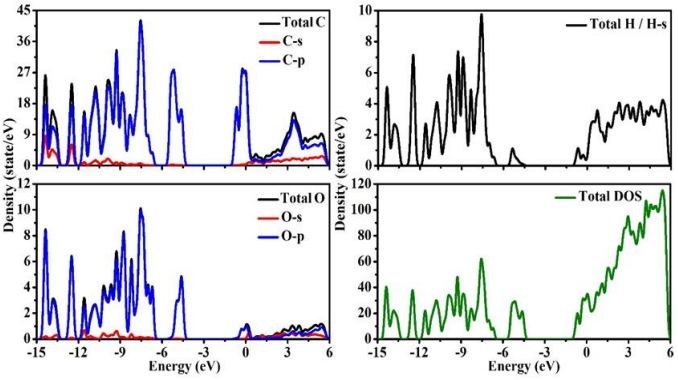


**Figure 7** TDOS and PDOS of C6

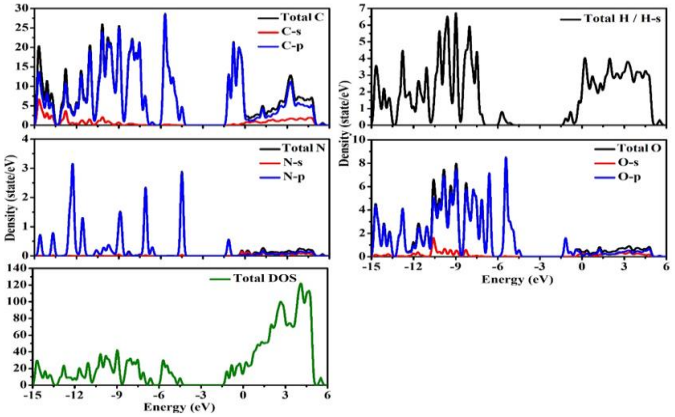


**Figure 8** TDOS and PDOS of C4-PABA

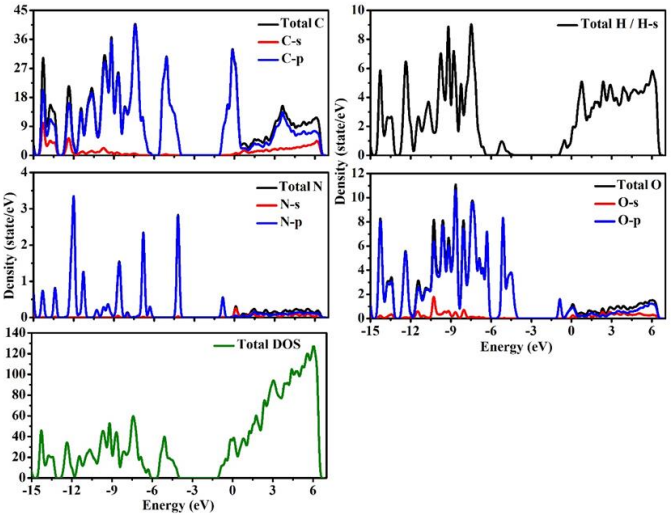


**Figure 9** TDOS and PDOS of C6-PABA

The contributions of each atom in the conduction and valence bands are determined based on the graph of DOS by observing the peaks in both bands [34]. C4 and C6 show the same behavior, whereas C4-PABA and C6-PABA complexes demonstrate the same behavior. For PABA, C-p orbitals contribute the most in the conduction band, followed by H-s, O-p, and N-p orbitals. The same goes for the valence band, C-p orbitals show the main contributions. The contributions are followed by O-p, N-p, and H-s orbitals with less contribution. For C4 and C6, C-p orbitals contribute the most in the conduction band, followed by H-s and O-p orbitals. Their contributions in the conduction band are similar to those in the valence band. However, the contributions of O-p are slightly higher than those of H-s in the valence band. For the C4-PABA and C6-PABA complexes, the contribution shown by the atoms in the conduction band is in descending order from the C-p, H-s, O-p, and N-p orbitals. In the valence band, C-p orbitals denote the main contribution, followed by O-p, H-s, and N-p with minor contributions.

The results show that C contributes the most in both the conduction and valence bands. For atoms with both s and p electron-occupied orbitals, the p orbitals contribute significantly more than the s orbitals, as reported by Wu and co-workers [63]. The dominant behavior shown by C in the contribution of the band structure is also reported by previous studies [63], [64]. Based on the investigation of electronic structure, the outstanding contribution denoted by C is because of its special electron configuration [65].

## 4. CONCLUSION

The negative values obtained in the binding energy calculation show that both C4 and C6 can form stable structures with PABA. On the other hand, the decrease in band gap shown by the calixarene-PABA complexes compared to calixarenes and PABA molecules denotes a promising reactivity of these host and guest molecules. By the way, the band gap reduction shown by the C4-PABA and C6-PABA might be investigated in the coming days to explore their potential applications in other fields besides drug sensors. These findings indicate an excellent sensing

ability of C4 and C6 towards the PABA drug. Thus, it is anticipated that the findings of this study may be implemented in the creation of PABA nanosensors for medical and pharmaceutical applications in the near future.

## ACKNOWLEDGMENTS

This study was financially supported by the Sultan Idris Education University (UPSI) under the Fundamental Research Grants Scheme 2020-0256-103-02 (FRGS/1/2020/STG07/UPSI/02/2) provided by the Ministry of Higher Education Malaysia. The authors express gratitude to all parties involved in giving recommendations and assistance to complete this study.

## REFERENCES

[1] F. L. Supian, T. H. Richardson, A. V. Nabok, M. Deasy, and M. S. M. Azmi, "Adv. Mater.," vol. 895, pp. 520-525, 2014.
[2] Z. Liu, S. K. M. Nalluri, and J. Fraser Stoddart, "Chem. Soc. Rev.," vol. 46, no. 9, pp. 2459–2478, 2017.
[3] T. D. Moseev et al., "RSC Adv.," vol. 11, no. 11, pp. 6407–6414, 2021.
[4] R. Kumar et al., "Chem. Rev.," vol. 119, no. 16, pp. 9657–9721, 2019.
[5] N. A. Azahari, F. L. Supian, T. H. Richardson, and S. A. Malik, "Adv. Mater.," vol. 895, pp. 8-11, 2014.
[6] F. L. Supian, D. L. C. Kheng, and A. S. Razali, "Sains. Malays.," vol. 46, no. 1, pp. 91-96, 2017.
[7] F. L. Supian et al., "Langmuir," vol. 26, no. 13, pp. 10906–10912, 2010.
[8] S. Pawar, P. Shende, and F. Trotta, "Int. J. Pharm.," vol. 565, no. 333, pp. 333-350, 2019.
[9] J. Yang et al., "J. Chromatogr. A," vol. 1602, pp. 150-159, 2019.
[10] S. A. Perdomo et al., "Ieee Trans. Instrum. Meas.," vol. 70, no. 1, pp. 1-10, 2021.
[11] C. Maynard, I. Cummins, J. Green, and D. A. Weinkove, "BMC Biol.," vol. 16, no. 1, pp. 1-10, 2018.
[12] B. Marbois et al., "J. Biol. Chem.," vol. 285, no. 36, pp. 27827–27838, 2010.
[13] M. W. Mann and D. L. Popkin, "Handbook of Dermatology: A Practical Manual," John Wiley & Sons, 2019.
[14] A. N. M. Alamgir, "Therapeutic Use of Medicinal Plants and Their Extracts," Springer, 2018.
[15] C. A. Mutch et al., "ACS Infect. Dis.," vol. 4, no. 7, pp. 1067–1072, 2018.
[16] C. T. L. Chan et al., "Phys. Chem. Chem. Phys.," vol. 22, no. 15, pp. 8006–8020, 2020.
[17] H. L. Nguyen and J. A. Yiannias, "Clin. Rev. Allergy Immunol.," vol. 56, no. 1, pp. 41–59, 2019.
[18] S. Onoue et al., "J. Dermatol. Sci.," vol. 85, no. 1, pp. 4-11, 2017.
[19] J. Gardner, "Vibrational Healing through the Chakras: With Light, Color, Sound, Crystals and Aromatherapy," Crossing Press, 2014.
[20] H. Wu et al., "Langmuir," vol. 36, no. 5, pp. 1235–1240, 2020.
[21] C. Liu et al., "ACS Appl. Mater. Interfaces," vol. 10, no. 42, pp. 36229–36239, 2018.
[22] H. S. Yu, S. L. Li, and D. G. Truhlar, "J. Chem. Phys.," vol. 145, no. 13, p. 130901, 2016.
[23] W. Kohn, "Rev. Mod. Phys.," vol. 71, no. 5, p. 1253, 1999.
[24] M. Afsary, M. Bathaee, F. Bakhshinezhad, A. T. Rezakhani, and A. Bahrampour, "Phys. Rev. A," vol. 101, no. 1, p. 013403, 2019.
[25] P. A. Burr, E. Kardoulaki, R. Holmes, and S. C. Middleburgh, "J. Nucl. Mater.," vol. 513, p. 45-55, 2019.
[26] H. Shi, D. Han, S. Chen, and M. Du, "Phys. Rev. Mater.," vol. 3, no. 3, p. 034604, 2019.
[27] R. Ghafelehbashi et al., "Mater. Sci. Eng. C," vol. 109, p. 110597, 2020.
[28] P. Xu et al., "J. Phys. Chem. B," vol. 125, no. 2, pp. 601–611, 2021.
[29] G. A. Evingür and Ö. Pekcan, "Compos. Struct.," vol. 183, pp. 212–215, 2018.
[30] D. A. Abanin, A. V. Shytov, and L. S. Levitov, "Phys. Rev. Lett.," vol. 105, no. 8, p. 086802, 2010.
[31] I. Loa et al., "Phys. Rev. Mater.," vol. 2, no. 8, p. 085405, 2018.
[32] A. Kumar et al., "Phys. Rev. B," vol. 94, no. 18, p. 180105, 2016.
[33] K. Ahmad Shah, F. Ahmad Khanday, "Nanoscale Electronic Devices and Their Applications," CRC Press, 2020.
[34] R. Hu and J. Shang, "Appl. Surf. Sci.," vol. 496, p. 143659, 2019.
[35] X. Xu, X. Wang, and D. E. Jiang, "J. Phys. Chem. Lett.," vol. 12, no. 10, pp. 2484–2488, 2021.
[36] M. Morimoto et al., "Nat. Catal.," vol. 3, no. 12, pp. 969–984, 2020.
[37] P. Giannozzi et al., "J. Phys. Condens. matter," vol. 21, p. 395502, 2009.
[38] A. Dal Corso, "Comput. Mater. Sci.," vol. 95, pp. 337-350, 2014.
[39] G. Schmitz and J. Elm, "ACS Omega," vol. 5, no. 13, pp. 7601–7612, 2020.
[40] A. Altun, F. Neese, and G. Bistoni, "J. Chem. Theory Comput.," vol. 15, no. 1, pp. 215–228, 2019.
[41] R. K. K. Sanku et al., "Inclusion Complexes in Drug Delivery and Drug Targeting: Formation, Characterization, and Biological Applications," in "Targeted Nanosystems for Therapeutic Applications: New Concepts, Dynamic Properties, Efficiency, and Toxicity," M. A. Ilies and K. Sakurai, Eds., American Chemical Society, 2019, pp. 187-221.
[42] J. Wang, X. Ding, and X. Guo, "Adv. Colloid Interface Sci.," vol. 269, pp. 187–202, 2019.
[43] J. Guschlbauer et al., "Dalt. Trans.," vol. 48, no. 29, pp. 10971–10978, 2019.
[44] F. Ullah et al., "New J. Chem.," vol. 43, no. 15, pp. 5727–573, 2019.
[45] H. Sajid, T. Mahmood, and K. Ayub, "Synth. Met.," vol. 235, pp. 49–60, 2018.
[46] M. Zeeshan et al., "Chinese J. Chem.," vol. 39, no. 9, pp. 2391–2402, 2021.
[47] O. Lenchuk, P. Adelhelm, and D. Mollenhauer, "Phys. Chem. Chem. Phys.," vol. 21, no. 35, pp. 19378–19390, 2019.

[48] P. H. Joo and K. Yang, "Mol. Syst. Des. Eng.," vol. 4, no. 4, pp. 974–982, 2019.
[49] D. Çakır, C. Sevik, O. Gülseren, and F. M. Peeters, "J. Mater. Chem. A," vol. 4, no. 16, pp. 6029–6035, 2016.
[50] H. Zhang, Z. Wang, J. Ren, J. Liu, and J. Li, "Energy Storage Mater.," vol. 35, pp. 88–98, 2021.
[51] P. K. Lo and M. S. Wong, "Sensors," vol. 8, no. 9, pp. 5313–5335, 2008.
[52] L. Troian-Gautier et al., "R. Soc. Chem.," vol. 18, no. 19, pp. 3624–3637, 2020.
[53] M. Y. Zhang and H. Jiang, "Phys. Rev. B," vol. 100, no. 20, p. 205123, 2019.
[54] P. Borlido et al., "J. Chem. Theory Comput.," vol. 15, no. 9, pp. 5069–5079, 2019.
[55] M. Kolos and F. Karlický, "Phys. Chem. Chem. Phys.," vol. 21, no. 7, pp. 3999–4005, 2019.
[56] M. A. Kassem, A. Abu El-Fadl, A. M. Nashaat, and H. Nakamura, "J. Alloys Compd.," vol. 790, pp. 853–862, 2019.
[57] J. N. Lalena, D. A. Cleary, and O. B. M. H. Duparc, "Principles of Inorganic Materials Design," John Wiley & Sons, 2020.
[58] J. Yang et al., "Electrochem. commun.," vol. 96, pp. 22–26, 2018.
[59] J. B. Raoof, R. Ojani, E. Hasheminejad, and S. Rashid-Nadimi, "Appl. Surf. Sci.," vol. 258, no. 7, pp. 2788–2795, 2012.
[60] B. Tang, J. Zhao, J. F. Xu, and X. Zhang, "Chem. Sci.," vol. 11, no. 5, pp. 1192-1204, 2020.
[61] N. Yuksel, A. Köse, and M. F. Fellah, "J. Incl. Phenom. Macrocycl. Chem.," vol. 101, no. 1, pp. 77–89, 2021.
[62] A. Radzwan et al., "Comput. Condens. Matter.," vol. 24, pp. e00477, 2020.
[63] B. Wu et al., "Angew. Chemie - Int. Ed.," vol. 60, no. 9, pp. 4815–4822, 2021.
[64] P. N. O. Gillespie and N. Martsinovich, "ACS Appl. Mater. Interfaces," vol. 11, no. 35, pp. 31909–31922, 2019.
[65] W. Wu, S. Gong, and Q. Sun, "Diam. Relat. Mater.," vol. 108, pp. 107990, 2020.